Vol 11 No 2, February 2002
1009-1963/2002/11(02)/0132-07

Chinese Physics

© 2002 Chin. Phys. Soc.
and IOP Publishing Ltd

Investigation of titanium nitride coating by broadband laser ultrasonic spectroscopy

Gao Wei-Min(高伟民)[a)b)†], Christ Glorieux[a)c)], Walter Lauriks[a)], and Jan Thoen[a)]

[a)] *Laboratorium voor Akoestiek en Thermische Fysica, Departement Natuurkunde, Katholieke Universiteit Leuven, Celestijnenlaan 200D, B-3001 Leuven, Belgium*

[b)] *Lithography Department, Silicon Process Technology Division, Imec, Kapeldreef 75, B-3001 Leuven, Belgium*

[c)] *Postdoctoral Researcher for Fonds voor Wetenschappelijk Onderzoek-Vlaanderen, Belgium*

(Received 2 August 2001; revised manuscript received 10 October 2001)

We present a laser ultrasonic method to investigate a titanium nitride (TiN) coating specimen. The technique is based on the principle of surface acoustic wave (SAW) dispersion during acoustic propagation on a half-space with the presence of a thin layer. Due to the high efficiency of laser line-source excitation, we have been able to generate and detect a SAW with an excellent signal-to-noise ratio in a wide frequency band. An inverse fitting algorithm was employed to extract simultaneously the thickness and the elastic parameters of the TiN coating from the experimental SAW velocity dispersion curve.

Keywords: surface acoustic wave, laser ultrasonics, thin film, inverse problem
PACC: 4335, 4262

1. Introduction

Rayleigh waves, propagating on the free surface of an elastic half space, are well known. If the medium is homogeneous and isotropic, the velocity of the Rayleigh wave depends only on the elastic constants of the medium and not on the wavelength (or frequency), i.e. the Rayleigh wave is non-dispersive. The power density of the wave decays exponentially from the surface with a characteristic penetration depth of the order of a wavelength. Based on this principle, it is not difficult to understand that, in the presence of a thin coating on the substrate surface, the phase velocity of the corresponding quasi-Rayleigh waves will exhibit dispersion. In the high-frequency (or short wavelength) region, the wave velocity is only influenced by the coating. In the low-frequency region the wave velocity is dominated by the substrate. In the intermediate region the velocity behaviour reflects the transition of effective material properties between the two media. Therefore, the broadband surface acoustic wave (SAW) spectroscopy can be a suitable tool to investigate the properties of coatings and their bonding quality.

Many authors[1−3] have studied the propagation of a quasi-Rayleigh wave on the half space in the presence of a thin layer. The key problem is the determination of the dispersion of the phase velocity. Theory shows that, for a weak acoustic absorber, the variation of the phase velocity with frequency depends on the density, Young's modulus and Poisson's ratio of the coating and the substrate, as well as on the thickness of the coating. Taking into account the equations of wave motion and the boundary conditions for the coating surface and the interface between the coating and the substrate, the theoretical dispersion curve can be numerically calculated. By fitting this theoretical curve to experimental data, information on the elastic properties of the coating can be obtained. In order to obtain such information of an ultra thin coating, an ultra broadband dispersion curve is required. Measuring the SAW with conventional piezoelectric transducers, one may have higher frequencies, but can never obtain a very large bandwidth. However, the recently developed laser ultrasonics can achieve such a requirement by using ultrashort pulse laser generation and the respective detection technique. Another advantage of laser utrasonics is that the technique is a non-destructive and non-

† Author to whom correspondence should be addressed.
E-mail: Weimin.gao@imec.be Tel.:+32-16-281094. Fax:+32-16-281214.

contact technique. Its applications in coating investigations have been seen in various publications.[4–6] Lorenz *et al.*[7] have studied the dispersion features of the "stiffening" coating (the presence of the coating increases the SAW velocity above the Rayleigh velocity on the substrate) and the "loading" coating (the SAW velocity decreases by the presence of the coating). The same features were also demonstrated in the study of a coating of nickel and TiC on the substrate of a cemented carbide.[8] Kuschnereit *et al.* have studied the properties of a hot-filament-deposited polycrystalline diamond film on silicon[9] and of an ultra thin hydrogenated silicon film on fused silica.[10] In their measurements, the SAW was excited by a 7ns pulsed laser and the detection was performed by a polyvinylidene fluoride (PVDF) transducer fixed on a sharp metal wedge attached on the sample surface. This type of set-up is a half-optical method. A similar method was also employed by Schneider *et al.*[11] to characterize the plasma-sprayed ZrO_2 coating, and by Wu *et al.*[12] to determine the thickness and elastic properties of a bonding layer.

In this paper, we aim to characterize a TiN coating deposited on a steel substrate. There are many positive features of TiN material, such as: its extreme hardness (harder than carbide); wear resistance; corrosion resistance; high melting point; its resistance to nearly all chemicals; the fact that it is non-toxic and safe for the environment; and its attractive metallic gold coloration. These features make TiN widely preferred in many applications in various fields, ranging from tools to decorative coatings and from barrier layers to optical devices. Especially in the tool industry, the cutting efficiency can be significantly increased by using TiN coatings, which provide sharp edges or corners with extreme hardness and prevent galling, seizing or cold-welding in the cutting process. Therefore, the characterization of mechanical properties of TiN coatings is an important and challenging problem. Different techniques, including conventional ultrasonics, exist in the field of materials science for measuring the elastic properties of bulk solids and coatings. However, techniques such as leaky SAW,[13] acoustic microscopy,[14] auger electron spectroscopy,[15] x-ray diffraction[15] and Brillouin scattering,[16] all suffer from limited feasibility, because they are either destructive or require contact or a special treatment of the specimen. In this paper, we have employed an established all-optical laser ultrasonics set-up[17] to investigate the TiN coatings. We found that the thickness and the effective Rayleigh velocity of the coating can be estimated simultaneously by inversely fitting the measured SAW dispersion relation.

2. Theoretical model of coating-substrate system and the inverse fitting procedure

2.1. Exact theoretical model of SAW in a coating-substrate system

Figure 1 shows the coordinate axes of a thin film, with a thickness H, coated on a half-space substrate. A plane SAW (y–z plane) propagates along the x-direction and penetrates over a finite extent in the y-direction with a depth of the order of a wavelength. The coating, which has different densities and elastic constants compared to the substrate, is assumed to be perfectly bonded on the substrate. According to the basic theory of elasticity, the equation of motion with respect to the potentials can be decomposed into two equations

$$(\lambda + 2\mu)\nabla^2\phi = \rho\ddot{\phi}, \tag{1}$$

$$\mu\nabla^2\psi = \rho\ddot{\psi}, \tag{2}$$

where the scalar potential ϕ, $\nabla \cdot \nabla\phi = \nabla^2\phi$, and the vector potential ψ, $\nabla \cdot \nabla \times \psi = 0$, refer to the propagation of longitudinal and shear waves, respectively.

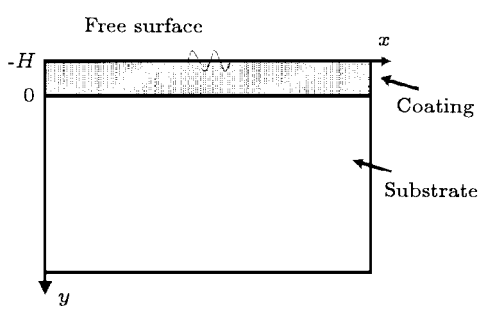


Fig.1. The coordinates of the system: a thin film with a thickness H coated on a half-space substrate. A plane SAW (y–z plane) propagates along the x-direction.

According to the above assumptions of the SAW in the considered coating-substrate system, the solutions of Eqs.(1) and (2) must have the forms

$$\phi = \Phi(y)\exp(\mathrm{i}qx - \mathrm{i}\omega t), \tag{3}$$

$$\psi = \Psi(y)\exp(\mathrm{i}qx - \mathrm{i}\omega t), \tag{4}$$

where $i = \sqrt{-1}$, q is the wavenumber of the guided wave and ω is the angular frequency.

For the substrate medium (the respective expressions of the displacement and the stress are denoted by the index "s"), the conditions of finiteness at infinity[18] still hold since we consider that the waves are SAW propagating on a half space. The respective equations can be written, with the adaptation of the notations in the present system, as follows

$$2\mathrm{i}qp_{\mathrm{ls}}u_{xs}(0)+(p_{\mathrm{ts}}^2+q^2)u_{ys}(0)+\frac{p_{\mathrm{ls}}}{p_{\mathrm{s}}\nu_{\mathrm{ts}}}\sigma_{yys}(0)+\frac{\mathrm{i}q}{\nu_{\mathrm{ts}}^2\rho_{\mathrm{s}}}\sigma_{yxs}(0)=\frac{q_{\mathrm{ls}}^2}{\nu_{\mathrm{ts}}^2}G_{\mathrm{s}}(p_{\mathrm{ls}}), \quad (5)$$

$$(p_{\mathrm{ts}}^2+q^2)u_{xs}(0)-2\mathrm{i}qp_{\mathrm{ts}}u_{ys}(0)-\frac{\mathrm{i}q}{\nu_{\mathrm{ts}}^2\rho_{\mathrm{s}}}\sigma_{yys}(0)+\frac{p_{\mathrm{ts}}}{\rho_{\mathrm{s}}\nu_{\mathrm{ts}}^2}\sigma_{yxs}(0)=0. \quad (6)$$

The coating (the expressions of the displacement and the stress are denoted by the index "c") is considered to be a thin waveguide. Thus Eqs.(3) and (4) can be further written as

$$\phi=(A\cosh(p_{\mathrm{lc}}y)+B\sinh(p_{\mathrm{lc}}y))\exp(\mathrm{i}qx-\mathrm{i}\omega t), \quad (7)$$

$$\psi=(C\cosh(p_{\mathrm{tc}}y)+D\sinh(p_{\mathrm{tc}}y))\exp(\mathrm{i}qx-\mathrm{i}\omega t), \quad (8)$$

where $p_{\mathrm{lc}}^2=q^2-q_{\mathrm{lc}}^2$, $p_{\mathrm{tc}}^2=q^2-q_{\mathrm{tc}}^2$; $q_{\mathrm{lc}}=\omega/\nu_{\mathrm{lc}}$ is the longitudinal wavenumber and $q_{\mathrm{tc}}=\omega/\nu_{\mathrm{tc}}$ is the transverse wavenumber; ν_{lc} and ν_{tc} are the longitudinal velocity and the shear velocity for the coating material, respectively. The coefficients A, B, C and D are constants. These potential solutions render the displacement and stress profiles in the coating via the following fundamental relations

$$u_{xc}(y)=\frac{\partial\phi}{\partial x}-\frac{\partial\psi}{\partial y}, \quad (9)$$

$$u_{yc}(y)=\frac{\partial\phi}{\partial y}+\frac{\partial\psi}{\partial x}, \quad (10)$$

$$\frac{\sigma_{yxc}(y)}{\rho_{\mathrm{c}}\nu_{\mathrm{tc}}^2}=\frac{\partial u_{xc}(y)}{\partial y}+\frac{\partial u_{yc}(y)}{\partial x}, \quad (11)$$

$$\frac{\sigma_{yyc}(y)}{\rho_{\mathrm{c}}\nu_{\mathrm{lc}}^2}=\frac{\partial u_{yc}(y)}{\partial y}+\left(\frac{\nu_{\mathrm{lc}}^2-2\nu_{\mathrm{tc}}^2}{\nu_{\mathrm{lc}}^2}\right)\times\frac{\partial u_{xc}(y)}{\partial x}-\frac{G_{\mathrm{c}}(y)}{\nu_{\mathrm{lc}}^2}. \quad (12)$$

The term $G_i(y)$ in the above equations is related to the wave excitation source. We assume that it is only a function of y, which is reasonable for our experimental regime (see the next section). The boundary conditions of this coating-substrate system include: (a) the zero stress at the free coating surface, i.e. $\sigma_{yxc}(-H)=0$, $\sigma_{yyc}(-H)=0$; (b) the continuity of displacements and stresses at the coating-substrate interface, i.e. $u_{xs}(0)=u_{xc}(0)$, $u_{ys}(0)=u_{yc}(0)$, $\sigma_{yxs}(0)=\sigma_{yxc}(0)$, $\sigma_{yys}(0)=\sigma_{yyc}(0)$. There are four unknowns for each side of the interface (two components of the displacement and two components of the stress). For the coating medium, the four unknowns are represented by the four coefficients, A, B, C and D. Substituting the respective equations into the six boundary conditions, together with the two additional equations from the finiteness condition (Eqs.(5) and (6)), yields a system of 8×8 equations

$$L_{ij}\cdot X=G, \quad (13)$$

where $X=[u_{xs}(0),u_{ys}(0),\sigma_{yys}(0),\sigma_{xys}(0),A,B,C,D]^T$ (T is the transpose operator) represents the eight unknowns, G represents the source-related terms, L_{ij} is an 8×8 matrix which is a function of the densities and the bulk velocities of the coating and the substrate media, as well as the coating thickness. This theoretical model can be used to make the forward numerical calculations of the phase velocity dispersion. Since only the roots of the solutions lead to surface wave-like solutions (inverse Laplace transform, residue theorem),[18] the set of equations in the determinant L_{ij} can be set to zero, i.e.

$$|L_{ij}|=0, \quad (14)$$

yielding the dispersion $q(\omega)$ and thus $\nu(\omega)$, for a specific coating-substrate medium and a given coating thickness. Equation (14) is solved using a root-searching algorithm which finds the root of the equations for every given frequency. When multiple roots are present, only the one yielding substrate wavenumbers which fulfil the finiteness conditions is retained. In fact, we prefer this exact theoretical model to a more approximate method[1,3] because it can be easily extended to the study of multilayer samples.[19]

2.2. Inverse fitting procedure

The aim of the laser ultrasonics SAW measurements in this study is to estimate the thickness and the bulk velocities of the coating deposited on a known substrate. This is achieved by using a nonlinear inversion algorithm, which fits the numerical velocity dispersion curves using the exact theoretical model for the elastic parameters to those of measurements. This procedure can be formulated as

$$\chi_\gamma^2=\frac{1}{n-p}\sum_{j=1}^{n}\frac{[\nu_{\mathrm{fit}}(f_j,H,\nu_{\mathrm{lc}},\nu_{\mathrm{tc}},\rho_{\mathrm{c}})-\nu_{\mathrm{exp}}(f_j)]^2}{\sigma_j^2}\to\min, \quad (15)$$

where $\nu_{\rm exp}(f_j)$ is the experimental SAW velocity, $\nu_{\rm fit}(f_j, H, \nu_{\rm lc}, \nu_{\rm tc}, \rho_{\rm c})$ is the calculated velocity from Eq.(14), n represents the number of data points utilized in the inversion process, σ_j are the experimental standard deviations, and p is the number of fitting parameters. In fact, $\nu_{\rm fit}$ is a function not only of the coating parameters but also of the substrate parameters. Here we assume that the properties of the substrate are known in order to reduce the number of fitting variables. Since the bandwidth is always limited by the experimental conditions and the multi-parameter nonlinear fitting is trivial, the fitting parameters are strongly dependent on the quality of the measurement and on the experimental frequency band. Furthermore, the nonlinear multi-parameter fitting requires good initial estimates of some parameters, and some constraints are necessary for the numerical calculations. Once the best fitting parameters are found, the standard deviation of the fitting parameter can be related to the second derivative of the chi-square function with respect to that parameter. The best estimated value of this parameter occurs at the minimum chi-square point from the graph of chi-square versus the parameter, which is approximately parabolic. The confidence interval of the fitting parameter can be estimated by the interval for which the typical chi-square values are smaller than twice its minimum value.[20]

3. SAW measurement of the TiN coating sample

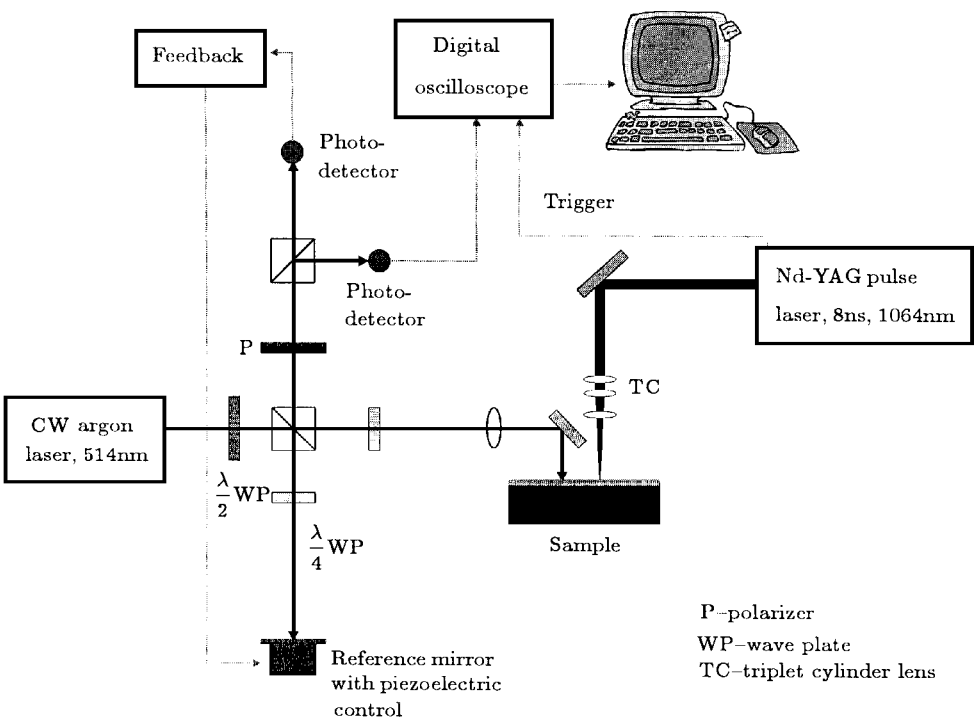


Fig.2. Schematic diagram of the laser ultrasonic spectroscopy set-up.

Two specimens are used in our study. They are 5mm thick tool steel substrates covered with polycrystalline TiN using the method of dc magnetron sputtering. This combination represents a "stiffening" situation in which the existence of the film increases the SAW velocity over that of the substrate when the frequency increases. Figure 2 shows the experimental set-up[17] used. A pulsed Nd:YAG laser (1064nm, 400mJ) with a duration of 8ns is used as the generation source. The pump beam is attenuated and focused by a triplet cylindrical lens into a thin long line ($\sim 20\mu$m wide and 15mm long). The generated SAWs travel in the direction perpendicular to the line source, and are detected at different distances from the source. The normal displacement is detected by a Michelson interferometer using a CW argon laser (514nm) beam focused to less than 5μm. One half-wave plate and two quarter-wave plates are placed in the optical paths as an optical filter in order to reduce the influence of spuriously reflected light and to balance the light of the two paths. An automatic feedback system using a piezoelectric element to position the reference mir-

ror has been designed to eliminate low-frequency environmental noise and to keep the system in the linear sensitivity range. After detection and amplification in a high-performance photodetector (femto current-amplifier photoreceiver with 0–200MHz bandwidth), the signals are sampled by a digital oscilloscope. The minimum detectable displacement of this laser ultrasonic system is 0.05nm.

4. Results and discussion

Figure 3 shows a typical set of detected time signals. In the presented measurements, the source–receiver distance changes with a 0.5mm increment over a total distance of 5mm. Performing a fast Fourier transform (FFT) on the SAW pulses, the phase velocity dispersion can be obtained from the relation: $\nu(f)=2\pi f \cdot \Delta x/\Delta\phi(f)$. The obtained dispersion results are plotted in Fig.4. For the sake of clarity, in Fig.4 the error bars are plotted only for one of the dispersion curves, while the other curve has similar errors. The velocity dispersion clearly exhibits an increasing behaviour when the frequency increases from 0 to 50MHz. As demonstrated in the figure, the dispersions of the two samples are different, which must be due to the difference in their elastic properties. In principle, the velocity should reach the Rayleigh wave velocity of TiN ($\sim$5400m$\cdot$s^{-1}) if the frequency is high enough where the wavelength is comparable with the coating thickness. Our results are somehow limited by the experimental bandwidth. The inverse fitting procedure was performed over the experimental results with three free parameters: the coating thickness H and the longitudinal and shear velocities of the coating. The other involved parameters were set to known values: the bulk velocities of the substrate ($\nu_{\rm ls}$=5900m$\cdot$s^{-1}, $\nu_{\rm ts}$=3310m$\cdot$s^{-1}), and the densities of both the substrate and the coating ($\rho_{\rm s}$=8055kg$\cdot$m^{-3}, $\rho_{\rm c}$=5220kg$\cdot$m^{-3}). The elastic parameters of the bulk substrate material are of minor importance and can easily be determined by other methods. We have taken these values from the literature and we do not believe that they deviate appreciably from the real values of the material, a typical high-speed tool steel. One might question why, in addition to the parameters of the substrate, the density of the coating is also predefined as a constant. This is because the deposition conditions of this specific TiN coating on our samples were identical, therefore the composition of the coatings is the same. This is unlike in some other studies where the coating density should be set as a fitting parameter since it changes with the variation of the process conditions. In our case, one less free parameter significantly reduced the difficulty of the fitting calculation. The best fitting results of the two samples are plotted in Fig.4.

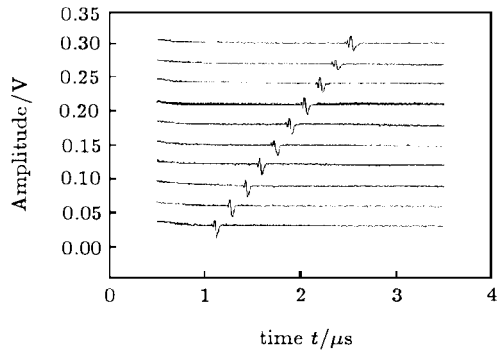


Fig.3. A typical set of detected time histories of SAW on a steel sample with a TiN coating.

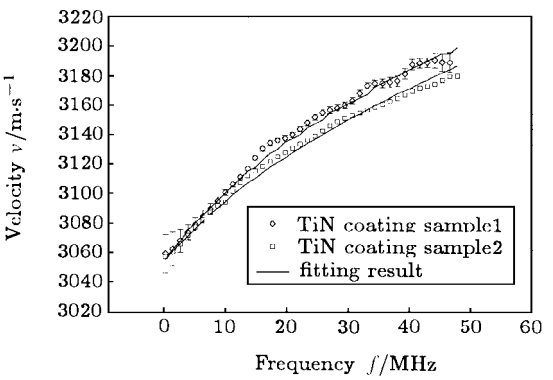


Fig.4. The experimental SAW dispersion and the fitting results.

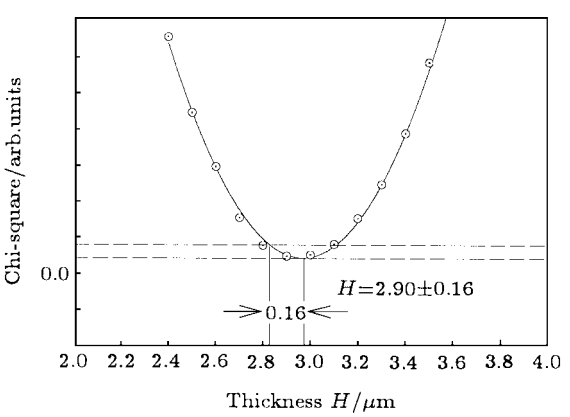


Fig.5. Dependence of the chi-square values on the coating thickness. The relationship shows that a clear single local minimum exists which indicates the best fitting result of the coating thickness.

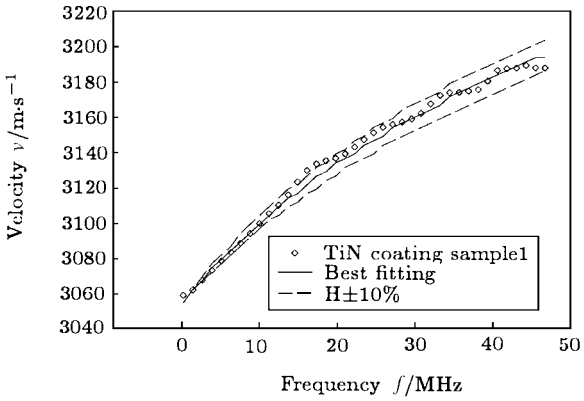


Fig.6. The best fitting curve and the curves with ±10% variations of coating thickness are plotted over the experimental curve.

Among the three fitting parameters (H, $\nu_{\rm l}$, $\nu_{\rm t}$), the thickness could be unambiguously determined. Figure 5 shows the dependence of the fitting quality, characterized by the chi-square value, on the coating thickness for one of the two samples measured. The relationship is parabolic with a clear single local minimum, indicating the best fitting result of the coating thickness. The error of the fitting result can be estimated by the interval corresponding to the double-minimum chi-square value. Figure 6 presents the fitting curve with respect to the obtained thickness value. In the figure, we also plot curves with 10% thickness variations, in which a clear deviation to the best result is demonstrated. The same effect is also seen in the plots for the respective longitudinal and shear velocities with 10% variation (Fig.7). However, instead of an expected localized minimum, a line of constant minima was found if the contour of the chi-square values is plotted versus $\nu_{\rm l}$ and $\nu_{\rm t}$ (Fig.8). This degeneracy is typical for Rayleigh waves in general: for example, for a semi-infinite medium Rayleigh velocity $\nu_{\rm r}$ depends both on $\nu_{\rm l}$ and $\nu_{\rm t}$, and these two bulk velocities cannot be separately deduced from $\nu_{\rm r}$. The extra information introduced by the coating dispersion is not sufficient to lift this degeneracy. A general knowledge of the Poisson ratio is needed to lift the degeneracy. This is illustrated in Fig.8. The Poisson ratio is directly linked to the ratio of shear and longitudinal velocities. The straight lines in the figure correspond to the curves of constant Poisson ratio. If the Poisson ratio is known, then plotting the corresponding curve together with the $\chi^2_\gamma(\nu_{\rm l},\nu_{\rm t})$ contour plot, the cross section of the curve with the contour line of χ^2_γ minima renders the $\nu_{\rm l}$ and $\nu_{\rm t}$ values. For the TiN coating, a Poisson ratio of 0.25 is close to its reported value and normally it remains quite constant.

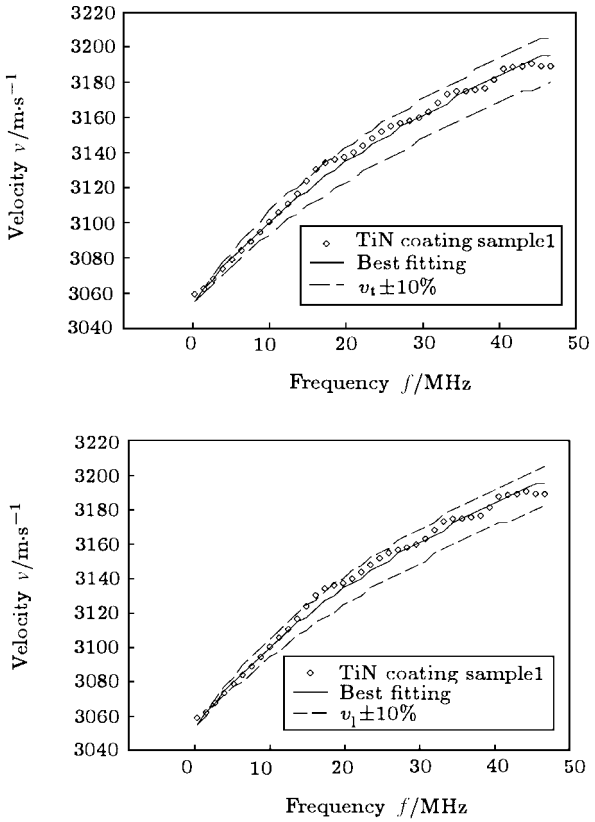


Fig.7. The fitting curves of the shear (top) and longitudinal (bottom) velocities with ±10% variations. The symbols represent the experimental data.

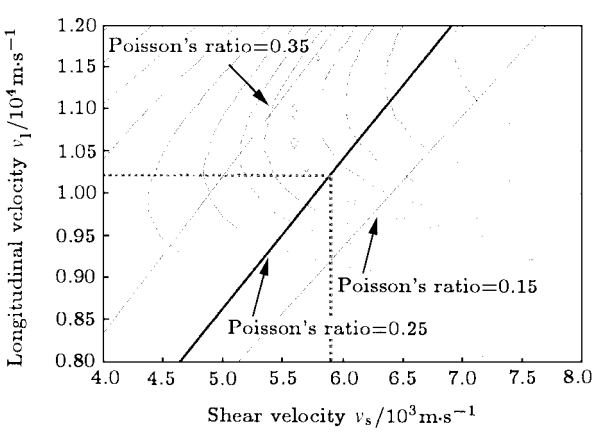


Fig.8. Contour plot of the chi-square values versus $\nu_{\rm l}$ and $\nu_{\rm t}$. The straight lines correspond to the relation of $\nu_{\rm l}/\nu_{\rm t}$ with a fixed Poisson ratio ν. The middle line with ν=0.25 leads to the fitting results of $\nu_{\rm l}$=10218m·s^{-1} and $\nu_{\rm t}$=5900m·s^{-1}.

We note that a typical coating-substrate dispersion curve is an S-like curve going from the Rayleigh velocity of the substrate in the low-frequency limit to the Rayleigh velocity of the coating in the high-frequency limit. The bending point of the S-curve is mainly determined by the thickness of the coating. So one can expect that, for a substrate-coating

sample, although the longitudinal and transverse velocities cannot be separately fitted from the dispersion curve, the "effective Rayleigh velocity" of the coating and substrate can be unambiguously determined. By the effective Rayleigh velocity, we mean the Rayleigh velocity of the (imagined) equivalent semi-infinite medium made of the coating with respect to the substrate material. As a result of Fig.8, we have found that indeed the effective Rayleigh velocities are equal to the line of minima, $(\nu_{\rm l}, \nu_{\rm t})_{\rm min}$ within experimental uncertainty.

In summary, the presented analytical method illustrates that, given a sufficiently wide bandwidth, the dispersion curves of quasi-Rayleigh waves for coating-substrate systems can unambiguously yield the values for the thickness and for the effective Rayleigh velocity of the coating (and substrate). The chi-squared analysis points out that the longitudinal and transverse velocities (and thus the complete set of elastic parameters) can only be unambiguously determined, provided that the Poisson ratio is known from other sources. Assuming a Poisson ratio ν=0.25 for TiN, we have obtained $\nu_{\rm l}$=10218m·s^{-1}, $\nu_{\rm t}$=5900m·s^{-1}, corresponding to a Young's modulus of Y=454GPa. Similar results ($\nu_{\rm l}$=10082m·s^{-1}, $\nu_{\rm t}$=5851m·s^{-1} and the corresponding Y=445GPa) were obtained for the TiN coating sample 2 (see Fig.4), except for a slightly larger thickness value ((3.1±0.2)μm compared to (2.90±0.16)μm for sample 1).

Acknowledgment

The authors would like to thank Dr Wu Pei-Qiang from Department of Metallurgy and Material Engineering, Catholic University of Leuven, Belgium, for providing the samples and related parameters.

References

[1] Tiersten H F 1968 *J. Appl. Phys.* **40** 770
[2] Farnell G W and Alder E L 1972 *Phys. Acous.* (New York: Academic) p 35
[3] Gusev V P and Hess H 1995 *Appl. Phys.* A **61** 299
[4] Stanislav I R and Matikas T E 1996 *J. Mater. Res. Soc. Bull.* October 22
[5] Coste J F 1997 *Ultrasonics* **35** 431
[6] Kuchler R and Richter E 1992 *Thin Solid Films* **315** 29
[7] Lorenz M, Vogel J A, Bruinsma A J A and Berkhout A J 1990 *Nondestruct. Test. Eval.* **5** 187
[8] Schneider D, Schwarz T and Schultrich B 1992 *Thin Solid Films* **219** 92
[9] Kuschnereit R, Hess P, Albert D and Kulisch W 1998 *Thin Solid Films* **312** 66
[10] Kuschnereit R, Fath H, Kolomenskii A A, Szabadi M and Hess P 1995 *Appl. Phys.* A **61** 269
[11] Schneider D, Schwarz T, Buchkremer H P and Stover D 1993 *Thin Solid Films* **224** 177
[12] Wu T T and Liu Y H 1999 *Ultrasonics* **37** 23
[13] Bogy D B and Gracewski S M 1983 *J. Acoust. Soc. Am.* **74** 591
[14] Zinin P, Lefevre O, Briggs G A D, Zeller B D, Cawley P, Kinloch A J and Thompson G E 1997 *J. Appl. Phys.* **82** 1031
[15] Elena M, Bonelli M, Bottani C E, Ghislotti G, Miotello A, Mutti P and Ossi P M 1993 *Thin Solid Films* **236** 209
[16] Every A G, Pang W, Comins J D and Stoddart P R 1998 *Ultrasonics* **36** 223
[17] Gao W M, Glorieux C, Kruger S E, Van de Rostyne K, Gusev V, Lauriks W and Thoen J 2001 *J. Mater. Sci. Eng.* A **313** 170
[18] Gusev V, Desmet C, Lauriks W, Glorieux C and Thoen J 1996 *J. Acoust. Soc. Am.* **100** 1514
[19] Glorieux C, Gao W M, Kruger S E, Van de Rostyne K, Lauriks W and Thoen J 2000 *J. Appl. Phys.* **88** 4394
[20] Glorieux C, Li Voti R, Thoen J, Bertolotti M and Sibilia C 1999 *Inverse Probl.* **15** 1149